EPJ Web of Conferences **198**, 00003 (2019) https://doi.org/10.1051/epjconf/201919800003
QTech 2018

New precise measurements of muonium hyperfine structure at J-PARC MUSE

P. Strasser[1,**], M. Abe[1], M. Aoki[2], S. Choi[3], Y. Fukao[1], Y. Higashi[4], T. Higuchi[4], H. Iinuma[5], Y. Ikedo[1], K. Ishida[6], T. Ito[7], T. U. Ito[8], M. Iwasaki[6], R. Kadono[1], O. Kamigaito[6], S. Kanda[6], K. Kawagoe[7], D. Kawall[9], N. Kawamura[1], M. Kitaguchi[10], A. Koda[1], K. M. Kojima[11], K. Kubo[12], M. Matama[7], Y. Matsuda[4], Y. Matsudate[4], T. Mibe[1], Y. Miyake[1], T. Mizutani[4], K. Nagamine[1], S. Nishimura[1], T. Ogitsu[1], N. Saito[1], K. Sasaki[1], S. Seo[4], H. M. Shimizu[10], K. Shimomura[1], T. Suehara[7], M. Tajima[4], K. S. Tanaka[13], T. Tanaka[4,14], J. Tojo[7], D. Tomono[15], H. A. Torii[16], E. Torikai[17], A. Toyoda[1], Y. Tsutsumi[7], K. Ueno[1], Y. Ueno[4], D. Yagi[4], A. Yamamoto[1], T. Yamanaka[7], T. Yamazaki[1], H. Yasuda[4,1], M. Yoshida[1], and T. Yoshioka[7], *on behalf of the MuSEUM Collaboration*

[1]High Energy Accelerator Research Organization (KEK), 1-1 Oho, Tsukuba, Ibaraki 305-0801, Japan
[2]Department of Physics, Osaka University, 1-1 Machikaneyama, Toyonaka, Osaka 560-0043, Japan
[3]Department of Physics, Seoul National University, Seoul 151-742, South Korea
[4]Graduate School of Arts and Sciences, University of Tokyo, 3-8-1 Komaba, Meguro-ku, Tokyo 153-8902, Japan
[5]Ibaraki University, College of Science, 2-1-1 Bunkyo, Mito 310-8512, Japan
[6]RIKEN, 2-1 Hirosawa, Wako, Saitama 351-0198, Japan
[7]Department of Physics, Kyushu University, 744 Motooka, Nishi, Fukuoka, Fukuoka 819-0395, Japan
[8]Advanced Science Research Center, Japan Atomic Energy Agency (JAEA), 2-4 Shirane Shirakata, Tokai-mura, Naka-gun, Ibaraki 319-1195, Japan
[9]Physics Department, University of Massachusetts Amherst, Amherst, MA, USA
[10]Department of Physics, Nagoya University, Nagoya 464-8602, Japan
[11]TRIUMF, Vancouver, BC V6T 2A3, Canada
[12]International Christian University (ICU), 3-10-2 Osawa, Mitaka, Tokyo 181-8585, Japan
[13]Cyclotron and Radioisotope Center (CYRIC), Tohoku University, 6-3 Aoba, Aramaki, Aoba-ku, Sendai, Miyagi 980-8578, Japan
[14]RIKEN, Cluster for Pioneering Research, 2-1 Hirosawa, Wako, Saitama 351-0198, Japan.
[15]Research Center for Nuclear Physics (RCNP), Osaka University, 10-1 Mihogaoka, Ibaraki, Osaka 567-0047, Japan
[16]Radioisotope Laboratory, Department of Chemistry, School of Science, The University of Tokyo, 7-3-1 Hongo, Bunkyo-ku, Tokyo 113-0033, Japan
[17]Interdisciplinary Graduate School of Medicine and Engineering, University of Yamanashi, 4-3-11 Takeda, Kofu, Yamanashi 400-8511, Japan

Abstract. High precision measurements of the ground state hyperfine structure (HFS) of muonium is a stringent tool for testing bound-state quantum electrodynamics (QED) theory, determining fundamental constants of the muon magnetic moment and mass, and searches for new physics. Muonium is the most suitable system to test QED because both theoretical and experimental values can be precisely determined. Previous measurements were performed decades ago at LAMPF with uncertainties

* Corresponding author: patrick.strasser(at)kek.jp

mostly dominated by statistical errors. At the J-PARC Muon Science Facility (MUSE), the MuSEUM collaboration is planning complementary measurements of muonium HFS both at zero and high magnetic field. The new high-intensity muon beam that will soon be available at H-Line will provide an opportunity to improve the precision of these measurements by one order of magnitude. An overview of the different aspects of these new muonium HFS measurements, the current status of the preparation for high-field measurements, and the latest results at zero field are presented.

1 Introduction

Muonium is a hydrogen-like atom made of a bound state of a positive muon and an electron. High precision measurements of the muonium ground state hyperfine structure (HFS) can be regarded as the most sensitive tool for testing quantum electrodynamics (QED), and for determining precisely fundamental constants of the muon magnetic moment and hence its mass. Muonium is the most suitable system to test QED because both theoretical and experimental values can be precisely determined. Indeed, hydrogen HFS is one the most precisely measured value with a precision 0.2 ppt [1], but the theoretical value is presently limited at 0.6 ppm [2] due to our knowledge of the proton internal structure. In contrast, the hyperfine structure of positronium, which is a bound state of a positron and an electron, is limited experimentally by its mean lifetime (i.e. 140 ns for ortho-positronium) and measured with an accuracy of only 3.3 ppm [3–5], while its theoretical value is calculated at a level of 1.1 ppm [6] with uncertainties from unknown nonlogarithmic higher-order terms. However, the muonium lifetime of 2.2 μs is long enough to precisely measure it, and its feature that neither of its constituents have an internal structure (pure leptonic system), it can be accurately calculated. The previous muonium HFS measurement at zero field [7] reached a precision of 310 ppb, while the one at high field [8] achieved 12 ppb, both performed at LAMPF and with experimental uncertainties mostly dominated by statistical errors. The current theoretical value of muonium HFS is 61 ppb [9], but it is reported that effort to reach 2 ppb level is in progress.

In addition to test QED, it should be noted that the experimental values of the muon magnetic moment and mass are still currently determined by the previous muonium HFS experiment at high field [8]. The magnetic moment ratio between muon and proton is of the utmost importance in the determination of the muon anomalous magnetic moment, also called muon g–2, and being regarded as a keystone at unravelling the physics of the standard model and beyond [10]. Furthermore, precision microwave spectroscopy of muonium can also contribute to many new physics such as testing CPT and Lorentz invariance incorporated in extensions to the standard model [11, 12], disentangling the proton radius puzzle [13, 14], searching for exotic particle [15, 16], and even probing for long-range neutrino-mediated forces [17].

The MuSEUM collaboration is now planning new and complementary measurements of the muonium HFS both at zero field and at a high magnetic field of 1.7 T. Our goal is to improve the precision of these measurements by one order of magnitude. The new high-intensity surface muon beamline, H-Line, that will soon be available at J-PARC MUSE [18], will provide an opportunity to achieve that goal. However, as we improve the statistics, understanding and suppressing systematic uncertainty become essential. Developments were performed and tools have been created to suppress uncertainties associated with the magnetic field inhomogeneity, muon stopping distribution, microwave power fluctuation and gas density extrapolation. An overview of the different aspects of these new precise muonium HFS measurements, the current status of the preparation for high-field measurements, and the latest measurements at zero field are presented.

2 Experimental method

The muonium ground state hyperfine splitting $\Delta\nu_{HFS}$ is to be measured by a microwave magnetic resonance technique. This transition will be measured directly at zero field and indirectly following the approach of the last experiment [8] at a static magnetic field of 1.7 T. The Breit-Rabi energy level diagram for muonium atom is shown in Fig. 1. The static field due to the Zeeman effect and the applied external RF field split the ground state of muonium into four different substates and the two spin-flip resonance frequencies ν_{12} and ν_{34} are measured. The sum of these two transition frequencies is constant, independent of the applied static field, and equal to the ground state hyperfine splitting at zero field, i.e., $\Delta\nu_{HFS} = \nu_{12} + \nu_{34}$, while the difference is directly related to the ratio of the muon and proton magnetic moments, i.e., $\mu_\mu/\mu_p \propto \nu_{34} - \nu_{12}$. Thus, the sum of the measured frequencies gives the QED test, while the difference is used to determine the values of the muon magnetic moment and mass.

The schematic view of the apparatus is shown in Fig. 2, and the experimental procedure can be summarized as follows: (1) muonium formation, (2) RF spin flip, and (3) positron asymmetry measurement. High-intensity pulsed surface muon (μ^+) beam, 100% backward polarized with respect of the muon momentum direction, are injected into a RF cavity located inside a gas chamber containing highly pure krypton gas. The profile of the incident muon beam is measured online by a non-destructive beam profile monitor located in front of the entrance window of the gas chamber. The μ^+ are stopped in Kr gas and rapidly form polarized muonium atom through a charge exchange reaction with Kr atoms. The muon spin can be flipped by applying a microwave magnetic field in the RF cavity perpendicular to the muon direction. The positrons (e^+) from muon decay are emitted preferentially in the direction of the muon spin. At the resonance, the RF field induces the muon spin flip changing the angular distribution of the emitted positrons from primarily backward to forward direction. Positrons are then detected with segmented scintillation detectors placed downstream of the gas chamber. Muonium spectroscopy is then performed by scanning the RF frequency and measuring positrons to determine resonance frequencies, i.e., $\Delta\nu_{HFS}$ at zero field and ν_{12} and ν_{34} at high field, respectively.

For zero-field measurements, the apparatus is enclosed in a magnetic shield box made of three layers of permalloy to suppress residual magnetic field. The experiment will be performed at the existing D-Line of the MUSE facility at J-PARC [18]. For high-field measurements, a large superconducting solenoid with an applied static field of 1.7 T

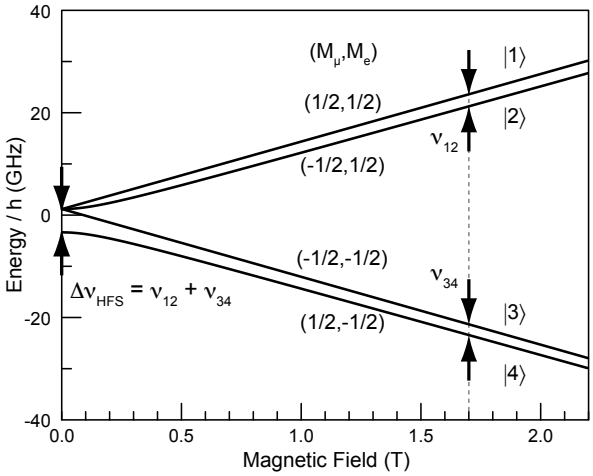

Fig. 1. Breit-Rabi energy level diagram for muonium atom under magnetic field.

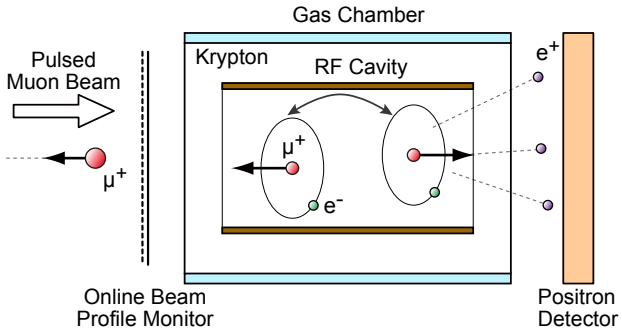

Fig. 2. Schematic view of the experimental setup. This apparatus is either enclosed in a magnetic shield box for zero-field measurements, or inserted in a large superconducting solenoid magnet for high-field measurements.

parallel to the muon momentum direction will be used. This static magnetic field and the introduced RF field in the cavity, perpendicular to the solenoid field, splits the ground state of the muonium into the four different substates as shown in Fig. 1. The high-intensity surface muon beam with an expected intensity of 1×10^8 μ^+/s will be provided by the new H-Line that is under construction at J-PARC MUSE.

3 Recent development and latest results

The progress of these new muonium HFS measurements is being reported regularly. The latest publications can be found in Ref. [19–22]. Here a brief overview of the different aspects of this experiment is presented focusing mainly on the recent developments: preparation for high-field measurements, latest measurements at zero field, and development of the time differential method.

3.1. Detector System

Several types of detectors are being used in these measurements. First, an online fiber beam profile monitor measures the muon beam pulse by pulse to suppress systematic uncertainty related to the muon beam profile and intensity stability [23]. Second, a 3D muon beam monitoring system was used offline to measure the muon beam stopping position in the Kr gas chamber at various gas pressure to reduce systematic uncertainty related to muonium atom distribution [20, 24]. Finally, an integrated highly-segmented scintillation detector system with high-rate capability is used to detect positrons [23, 25].

Recently, a new type of positron detector made of a highly-segmented silicon strip sensor with high-rate capability is being developed and tested [26]. Figure 3 shows a picture of this new integrated silicon strip detector. The silicon strip sensor has an active area of 97.28 mm square divided in two blocks with a thickness of 0.32 mm. The strip pitch and length are 0.19 mm and 48.575 mm, respectively. The number of strips is 512 × 2 blocks. The silicon strip sensor is connected on both sides though an adapter to two multi-Slit128A boards, where signals are directly processed by an analog/digital combined type integrated circuit. Each board contains four readout SliT128A chips, ASIC-based (Application Specific Integrated Circuit) ASD (amplifier-shaper-digitizer), that are controlled by an FPGA (Field Programmable Gated Arrays). This silicon strip detector was originally developed for J-PARC g−2/EDM experiment [10]. Details and performance of this new positron detector will be reported soon elsewhere.

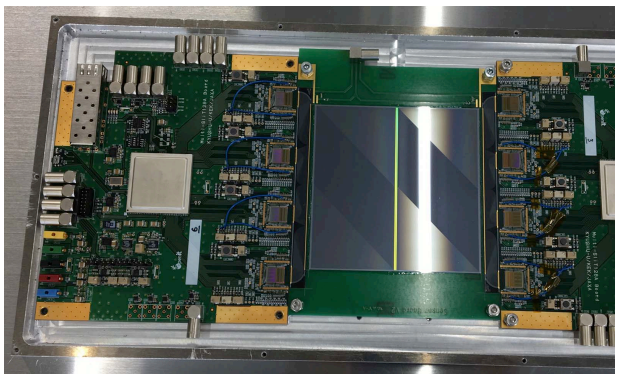

Fig. 3. Integrated silicon strip detector. The sensor is directly connected on both sides to an analog/digital combined type integrated circuit for readout and signal processing through four ASIC-ASDs (Slit128A) controlled by a FPGA.

3.2 Preparation for high-field measurements

High-field measurements will be performed with a superconducting solenoid magnet that was recycled from an old MRI magnet designed for high homogeneous magnetic field. The choice of a longer cavity to allow measurement at lower Kr gas density imposes strict requirements on the magnet. Indeed, the systematic uncertainty on the magnetic field was the second largest uncertainty in the previous experiment at LAMPF [8]. The muonium HFS frequency $\Delta\nu_{HFS}$ ($= \nu_{12} + \nu_{34}$) is in principle independent of the magnetic field. However, μ_μ/μ_p ($= \nu_{34} - \nu_{12}$) is dependent on the magnetic field, and its inhomogeneity relates largely to the systematic uncertainty. But since both ν_{12} and ν_{34} are measured separately, a precise calibration is still required in both cases. The present requirements for the magnetic field are a homogeneity of < 1 ppm with absolute calibration in a spheroidal volume of Ø200 mm × 300 mm (muon stopping region), a field stability of 0.1 ppm/h, and an absolute calibration at 10 ppb level. Improvement of the homogeneity of the MRI magnet and development of NMR probes for field calibration is steadily in progress.

Commissioning test of the MRI magnet was performed. After several iterative shimming processes, a field homogeneity within 0.8 ppm peak-to-peak in the muon stopping spheroid was reached. The long-term stability was measured at 3 ppb/hour over a 10 days period. The helium evaporation rate was 3 L/day. All this fulfills our design values.

For the precise magnetic field monitoring, a continuous wave NMR (CW-NMR) system with a RF pickup coil is being developed for both g–2/EDM and MuSEUM experiments at J-PARC. A field mapping probe with 24 RF pickup coils is being constructed to scan the muon stopping spheroid inside the MRI magnet. Also, a cross calibration test is in progress at Argonne National Laboratory with the pulse-NMR probe used at the FermiLab muon storage ring experiment [28]. The magnetic field is measured at the same position by both probes. The development of the CW-NMR probe is reported in details in [22]. Preliminary measurements showed that a resolution of 18 ppb could be reached [27]. Recently, even better resolution was obtained, but the analysis is still in progress and the results will be published elsewhere.

3.3. Zero-field measurements

Commissioning test experiments at zero field are being performed since February 2016 at the D2 experimental area (D-Line) of the MUSE facility. These engineering runs are

crucial to test the different aspects of the apparatus and grasp possible problems to be overcome before the start of the high-field measurements. Zero-field measurements are also important because of different systematics from the magnetic field (negligible at zero field). Figure 4 shows the apparatus during one of the engineering runs. The residual magnetic field is suppressed below 100 nT by a magnetic shield made of three layers of 1.5-mm thick permalloy that enclose completely the gas chamber and RF cavity.

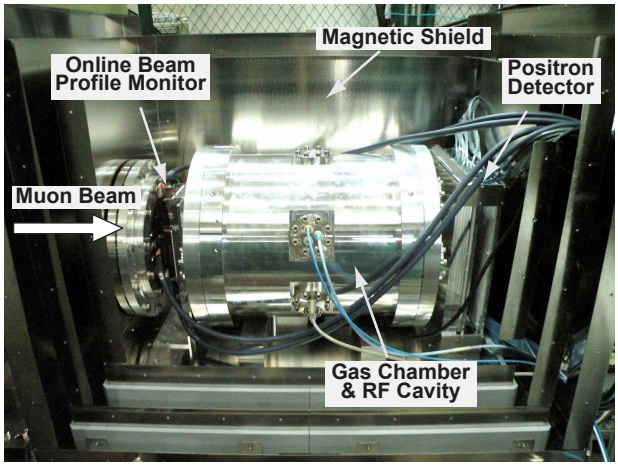

Fig. 4. Experimental setup for zero-field measurements at area D2 of MUSE D-Line.

Since the first resonance peak was observed in June 2016, systematic uncertainties due to gas pressure and impurity, RF power stability and muon beam profile distribution were studied. As we improve the statistics, the systematic uncertainty becomes more severe and needs to be carefully considered. It should be noted that our understanding of the systematical error in an experiment is limited by the time spent on the measurements, and that longer the measurement time, the lower the systematic uncertainty.

Figure 5 shows a typical resonance lineshape of the muonium HFS transition as a function of the applied RF frequency detuned from 4463.3 MHz measured in March 2018 (scintillation detector data). The time integral method is used by measuring alternatively RF ON and OFF at different detuning frequencies and taking the difference, i.e., $(N_{ON}-N_{OFF})/N_{OFF}$. The blue line shows a preliminary Lorentzian fitting result.

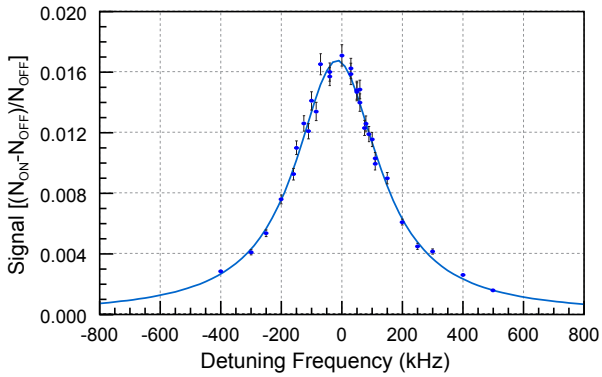

Fig. 5. Typical muonium HFS transition resonance lineshape as a function of the applied RF frequency detuned from 4463.3 MHz. The blue line shows a preliminary Lorentzian fitting result. The data analysis is in progress.

The transition frequency of muonium in gas varies with the gas pressure due to atomic collision between muonium and Kr. In March and June 2018, measurements were taken at lower Kr gas pressure (0.3, 0.4, 0.55 and 0.7 atm) in order to reduce the systematic uncertainty on the gas density extrapolation to the zero-density limit. Measurements at higher pressure (> 1 atm) are also being considered. We believe having reached a statistical precision better than the previous zero-field experiment at LAMPF of 1.4 kHz or 0.3 ppm [7]. The analysis is still on going and after considering carefully the systematic uncertainties the results will be reported in a later publication.

3.4 Time differential method

It was pointed out that the time differential method can in principle extract more information than the time integral method (or conventional method), but was unsuccessful in the previous measurements at LAMPF [8] because of low statistics.

The time differential method was developed and applied to muonium HFS measurements [26]. A realistic 3D simulation study was performed to assert its potential by using the actual calculated RF field distribution in the microwave cavity combined with the muon stopping distribution in the Kr gas chamber (i.e., muonium distribution). Figure 6 shows simulated results of the time differential signal for different detuning frequencies and fitted with an analytical function that contains the RF frequency and power as free fittings parameters. Each detuning frequency data are fitted individually, and the muonium HFS frequency can be determined with only one frequency data. The most sensitive detuning frequency is found at ~60 kHz, and the statistical uncertainty can be improved by 3.2 times compared to the conventional method. Also, this method can reduce systematics uncertainties of the RF power variation (free fitting parameter). This method requires however high-statistics data for fitting and an accurate determination of the time and number of detected positrons, thus a detector with high-rate capability and good time resolution is needed. This time differential method was used in the analysis of the silicon strip detector data and found to be very promising. The development is still on going.

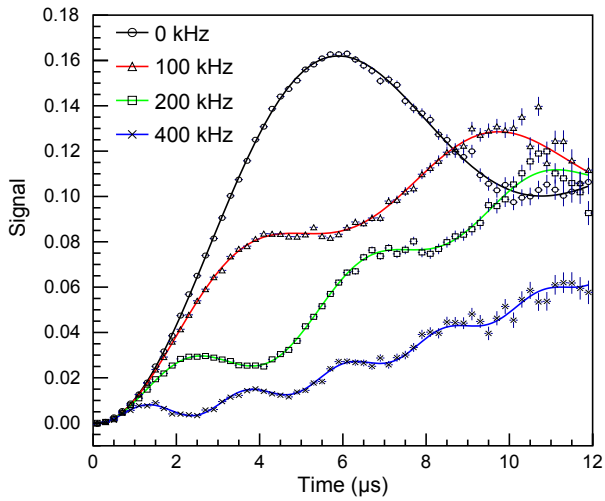

Fig. 6. Simulated time differential signals for different detuning frequencies. The solid lines represent fitting results with an analytical function that contains the RF frequency and power as free fittings parameters.

4 Summary

New precise muonium HFS measurements are important for further QED testing and new fundamental physics experiments. Improving the overall accuracy, estimating and understanding systematic uncertainties are essential in reaching that goal. Measurements at zero field are yielding their first results at MUSE D-Line. Preparation for the high-field measurements at H-Line is steadily progressing. At present, it is unclear when the new H-Line will be operational, but we are aiming at a first test experiment at high field sometime in 2019–2020.

This work was supported by the Grant-in-Aid for Scientific Research (A) from JSPS/MEXT KAKENHI grant numbers JP26247046 and JP17H01133.

References

[1] L. Essen *et al.*, Metrologia **9**, 128 (1973)
[2] M. Eides, H. Grotch, V.A. Shelyuto, *Theory of Light Hydrogenic Bound States*, Springer Tracts in Modern Physics **222** (Springer-Verlag, Berlin, Heidelberg, 2007), pp. 217–232
[3] M.W. Ritter *et al.*, Phys. Rev. A **30**, 1331 (1984)
[4] A.P. Mills, Phys. Rev. A **27**, 262 (1983)
[5] A. Ishida *et al.*, Phys. Lett. B **734**, 338 (2014)
[6] M. Baker *et al.*, Phys. Rev. Lett. **112**, 120407 (2014)
[7] D.E. Casperson *et al.*, Phys. Lett. B **59**, 397 (1975)
[8] W. Liu *et al.*, Phys. Rev. Lett. **82**, 711 (1999)
[9] P.J. Mohr, D.B. Newell, B.N. Taylor, Rev. Mod. Phys. **88**, 035009 (2016)
[10] M. Otani et al., JPS Conf. Proc. **8**, 025008 (2015)
[11] V.W. Hughes *et al.*, *The Hydrogen Atom: Precision Physics of Simple Atomic Systems,* Lecture Notes in Physics **570**, S.G. Karshenboim *et al.* (Eds.) (Springer-Verlag, Berlin, Heidelberg, 2001), pp. 397–406
[12] V.A. Kostelecky, A.J. Vargas, Phys. Rev. D **92**, 056002 (2015)
[13] R. Pohl et al., Nature 466, 213 (2010)
[14] S. J. Brodsy *et al.*, Phys. Rev. Lett. **94**, 022001 (2005)
[15] S. G. Karshenboim *et al.*, Phys. Rev. Lett. **104**, 220406 (2010)
[16] S. G. Karshenboim, V. V. Flambaum, Phys. Rev. A **84**, 064502 (2011)
[17] Y. V. Stadnik, Phys. Rev. Lett. **120**, 223202 (2018)
[18] H. Higemoto *et al.*, Quantum Beam Sci. **1**, 11 (2017)
[19] P. Strasser *et al.*, Hyperfine Interact. **237**, 124 (2016)
[20] Y. Ueno *et al.*, Hyperfine Interact. **238**, 14 (2017)
[21] K. Shimomura *et al.*, *Proc. of 7th Meeting on CPT and Lorentz Symmetry 2016* (World Scientific, Singapore, 2017), pp. 29-32
[22] T. Tanaka *et al.*, *Proc. of Int. Conf. on Precision Physics of Simple Atomic Systems (PSAS'2018)*, J. of Phys.: Conf. Ser. (to be published)
[23] S. Kanda *et al.*, PoS(**PhotoDet2015**)039 (2015)
[24] Y. Ueno *et al.*, JPS Conf. Proc. **18**, 011023 (2017)
[25] S. Kanda *et al.*, JPS Conf. Proc. **8**, 025006 (2015)
[26] S. Nishimura, Ph.D. Thesis, The University of Tokyo 2018 (unpublished)
[27] K. Sasaki *et al.*, IEEE Trans. Appl. Supercond. **26**, 0605604 (2016)
[28] G.W. Bennett *et al.*, Phys. Rev. D **73**, 072003 (2006)